Simultaneous Measurement of Recoil Velocity and Alignment of $S(^1D_2)$ Atoms in Photodissociation of OCS

Yuxiang Mo, Hideki Katayanagi, Michael C. Heaven,* and Toshinori Suzuki
Institute for Molecular Science, Myodaiji, Okazaki, 444 Japan
(Received 1 March 1996)

The recoil velocity and alignment of $S(^1D_2)$ atoms produced by ultraviolet photodissociation of OCS have been measured by a two-dimensional (2D) ion imaging method. The polarization dependence of the 2D images has been analyzed quantum mechanically, and helicity distributions have been determined for different velocity components of $S(^1D_2)$ atoms. The results show that the dissociation of $OCS \rightarrow CO(^1\Sigma^+) + S(^1D_2)$ occurs via two major pathways, and both of these processes produce the asymptotic states in A' and A'' symmetry. [S0031-9007(96)00608-4]

PACS numbers: 33.80.Gj, 33.80.Rv, 34.50.Lf, 34.50.Pi

Scalar and vector quantities of reaction products provide detailed insights into the dynamics of atomic or molecular collisions and molecular photodissociation. In particular, knowledge of vector quantities and their correlation is essential for the elucidation of stereochemical properties. In recent years, much attention has been paid to the correlation between the angular momentum ($\boldsymbol{J}$) and recoil velocity ($\boldsymbol{v}$) in photofragments [1,2]. The importance of $\boldsymbol{v}$-$\boldsymbol{J}$ correlation is that it is not lost by the formation of a long-lived collision complex, and that it serves as a versatile tool to probe the dynamics.

The $\boldsymbol{v}$-$\boldsymbol{J}$ correlation for a molecular fragment is mainly created by the repulsive force and torque at the bond cleavage. Therefore, it reflects the topography of the potential energy surface (PES), but it is not sensitive to electronic symmetry. On the other hand, the $\boldsymbol{v}$-$\boldsymbol{J}$ correlation in an atomic fragment is due to the electronic orbital alignment, so that it will reflect the electronic character of the PES. For example, in linear molecules the projection of electronic angular momentum onto the symmetry axis is a good quantum number. If the molecule dissociates along this axis, the projection of electronic angular momentum on the velocity axis (symmetry axis) is expected to be conserved during the dissociation.

Photodissociation often involves nonadiabatic transition(s) from an optically prepared state to some dark states. It is usually difficult to investigate the nature of these dark states. However, if electronic orbital alignment in atoms can provide information about the symmetry of these states, it will become an invaluable probe of dissociation dynamics.

Since the theoretical prediction made by Van Brunt and Zare in 1968 [3], the alignment of atoms produced by molecular photodissociation has been investigated [4–9]. These investigations were primarily concerned with overall alignment in the laboratory frame detected by polarized emission from atoms. Instead of observing emission, atomic fragments can be detected by resonance-enhanced multiphoton ionization (REMPI). REMPI allows us to examine not only the alignment from the polarization analysis, but also the velocity of atoms from ion imaging techniques [10] or time-of-flight measurements. Multiphoton excitation is also more advantageous than a one-photon process for extracting higher order terms in angular momentum polarization. Recently, Wang *et al.* [9] have shown that a one-dimensional time-of-flight spectrum of $Cl(^2P_{3/2})$ produced by 355 nm photodissociation of Cl_2 depends on the *probe* laser polarization. However, detailed information on the alignment has not been extracted [9]. In the present Letter, we describe a two-dimensional ion imaging method and quantum-mechanical analysis used to determine the alignment and the recoil velocity of atomic fragments simultaneously. The method allows us to observe $S(^1D)$ atoms produced with two different velocity components clearly, to examine their alignment in the molecular frame, and to discuss the electronic symmetry of the asymptotic state.

A supersonic molecular beam of OCS (10% in He) 1 mm in diameter was introduced parallel to the electric field vector of a time-of-flight mass spectrometer [10,11]. The molecular beam intersected with counterpropagated photolysis (223 nm) and probe laser beams at 79 mm downstream from the nozzle. Both of the laser beams were focused onto the molecular beam by axisymmetric lenses ($f = 300$ mm for photolysis and $f = 250$ mm for probe). The time delay between the photolysis and probe laser pulses was kept within 20 ns. Sulfur atoms were ionized by (2 + 1) REMPI using the resonance of $^1F_3 \leftarrow\leftarrow {}^1D_2$ at 288.19 nm, accelerated by electric fields, and projected onto a microchannel plate (effective diameter 38 mm) backed by a phosphor screen (P20). The transient image on the phosphor screen was monitored by a charge coupled device camera [$756\,(H) \times 581\,(V)$ pixels], and the video signal was integrated for 125 000–127 000 laser shots. The background pressures in the beam source and the main chamber, with a molecular beam on, were 2×10^{-5} and 2×10^{-7} Torr. The photolysis beam was the second harmonic of the output of a XeCl-pumped dye laser, while the probe beam was the second harmonic of the output of a YAG-pumped dye laser. Both of the laser beams were linearly polarized.

 0031-9007/96/77(5)/830(4)$10.00

The laser intensities used were 0.2 mJ/pulse (photolysis) and 0.1 mJ/pulse (probe). A double Fresnel rhomb was used to rotate laser polarizations. The probe laser frequency was scanned over the entire Doppler-broadened absorption line during the integration of images. The spatial resolution of the images was limited by the ratio of the size of the beam-laser interaction region (<1 mm) to the size of an image (~ 20 mm in diameter). The effective beam-laser interaction width is estimated to be much smaller than the molecular beam width, since (2 + 1) REMPI is most efficient in the laser beam waist at the molecular beam center. Any precession of the angular momentum about external magnetic (the Earth) or electric (repeller) fields can be neglected for the time delay (<20 ns) between photolysis and probe.

The two-dimensional (2D) ion images of $S(^1D_2)$ produced by 223 nm photodissociation of OCS are shown in Figs. 1(a)–1(d). Four sets of images were measured for polarization analysis. The effect of orbital alignment is most clearly seen by comparing Figs. 1(c) and 1(d) in which the photolysis laser polarization is set perpendicular to the imaging plane. The original photofragment density distribution is cylindrically symmetric around the polarization vector of the photolysis laser. If there is no alignment in atoms, the ion signal is proportional to the density of fragments, so that the ion image should be cylindrically symmetric around the center. The change of the image from Figs. 1(c) to Fig. 1(d) and also the symmetry breaking in Fig. 1(d) are due to orbital alignment in $S(^1D_2)$. Because the $^1F_3 \leftarrow\leftarrow {}^1D_2$ transition favors the probe laser polarization ($\boldsymbol{\varepsilon}_{\rm probe}$) aligned parallel to $\boldsymbol{J}$ vector, signal intensity is reduced when $\boldsymbol{\varepsilon}_{\rm probe}$ is set perpendicular to $\boldsymbol{J}$. In Fig. 1(d), it is seen that the signal intensity is reduced along the direction of probe laser polarization. This suggests $\boldsymbol{\varepsilon}_{\rm probe} \perp \boldsymbol{J}$ for the fragments moving parallel to $\boldsymbol{\varepsilon}_{\rm probe}(\boldsymbol{\varepsilon}_{\rm probe} \parallel \boldsymbol{v})$ and, therefore, $\boldsymbol{J} \perp \boldsymbol{v}$ as a preferential alignment in the S atom. In the same way, the $\boldsymbol{J} \perp \boldsymbol{v}$ alignment in the S atom is seen by the intensity reduction at the center of Fig. 1(c). Alignment effects have also been observed in the images of $O(^1D_2)$ produced by photodissociation of O_3 [12] and N_2O [13].

In Figs. 1(a) and 1(b), in which the photolysis laser polarization is parallel to the imaging plane, two velocity components are clearly seen [14]. One has fast speed and small angular anisotropy, while the other has slow speed and large anisotropy. In the following analysis, alignment is considered independently for the two velocity components.

In the case of diatomic molecular fragments produced by the photodissociation of triatomic molecules, a classical model of angular momentum and the assumption of complete $\boldsymbol{v} \perp \boldsymbol{J}$ correlation may be applied for the analysis of alignment [15]. For atoms, however, angular momentum ($\boldsymbol{J}$) must be treated quantum mechanically [16–20], since the magnitude of J is small. Neither is it possible to make an *a priori* assumption about the $\boldsymbol{v}$-$\boldsymbol{J}$ correlation. The correlation, which is implicit in the m distribution, must be extracted from the data.

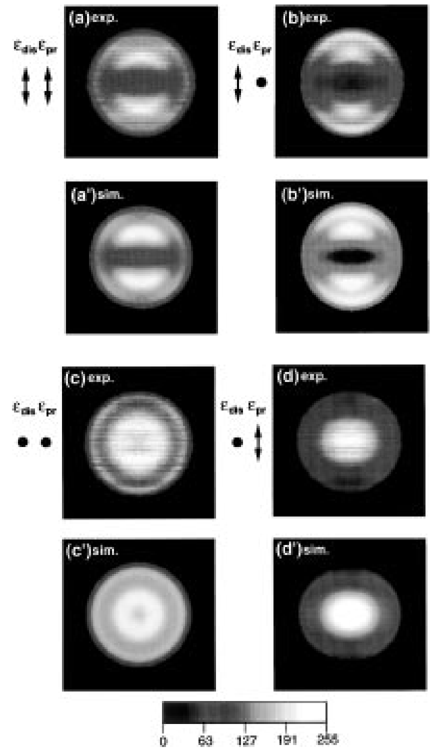

FIG. 1. 2D ion image of $S(^1D_2)$ produced by 223 nm photodissociation of OCS. (a), (b), (c), and (d) are the experimental data, and (a′), (b′), (c′), and (d′) are the simulated images obtained by using the parameters tabulated in Table I. The polarization direction of photolysis and probe laser beams are shown as $\varepsilon_{\rm dis}$ and $\varepsilon_{\rm pr}$. The experimental data have been symmetrized for ease of comparison with the calculated images. One of the original images without symmetrization can be found in Ref. [14].

The spatial distribution of photoions is determined by two factors,

$$\text{ion distribution} \propto I(\text{scat}) \times I(\text{det}),$$

where I(scat) is a differential cross section of photodissociation and I(det) is the ionization efficiency for photofragments. The differential cross section is expressed in space-fixed (SF) coordinates, with the Z axis defined along the photolysis laser polarization, by the following formula:

$$I(\text{scat}) = \frac{d^2\sigma}{dv\,d\Omega} = \frac{P_i(v)}{4\pi}[1 + \beta_i P_2(\cos\theta_t)] \quad (\text{for } i\text{th dissociation component}), \tag{1}$$

where $P(v)$ is a speed distribution, and β is an anisotropy parameter. The polar angle of recoil velocity in this frame is expressed by (θ_t, ϕ_t). The remaining task for us is to evaluate I(det) for each scattering angle (θ_t, ϕ_t) with explicit treatment of the $\boldsymbol{v}$-$\boldsymbol{J}$ correlation for S atoms.

The detection of reaction products by laser excitation is essentially the measurement of density. For a short *pump-probe* delay in photodissociation experiments, however, a density mode of detection is the same with a flux mode, since a laser pulse covers and detects all the velocity components equally. Hence, $I(\mathrm{det})$ is independent of speed v but proportional to the optical transition intensity. The two-photon absorption intensity for a linearly polarized probe laser beam is expressed in the probe laser photon (PR) frame, where the Z axis is defined along the polarization vector, by the following formula:

$$I(\mathrm{det}) \propto \sum_{k=0,2,4} P_k \rho_0^{(k)}(\mathrm{PR}), \tag{2}$$

where

$$P_k = \sum_m (-1)^{J_i - m} \sqrt{2k+1} \begin{pmatrix} J_i & k & J_i \\ -m & 0 & m \end{pmatrix} \left| \sum_{n_e, J_e} \frac{\langle n_f J_f m | r \cdot \hat{\varepsilon} | n_e J_e m \rangle \langle n_e J_e m | r \cdot \hat{\varepsilon} | n_i J_i m \rangle}{E_{n_e} - E_{n_i} - h\nu + i(\Gamma_e/2)} \right|^2$$

and $\rho_0^{(k)}(\mathrm{PR})$ are the multipole moments of the m population distribution. (:::) is $3j$ symbol, J_f, J_e, and J_i are the total angular momenta, n_f, n_e, and n_i denote all other quantum numbers for the final, virtual, and initial states, respectively. Γ_e is the homogeneous linewidth of the virtual state. m is the magnetic quantum number referenced to the photon frame. By neglecting the polarization effect for the ionization step in (2 + 1) REMPI, Eq. (2) is considered to be a detection efficiency of photofragments. Using the Wigner-Eckart theorem, P_k can be expressed as follows:

$$P_k = \sum_m (-1)^{J_i - m} \sqrt{2k+1} \begin{pmatrix} J_i & k & J_i \\ -m & 0 & m \end{pmatrix} \left| \sum_{J_e} (-1)^{J_f + J_e} \begin{pmatrix} J_f & 1 & J_e \\ -m & 0 & m \end{pmatrix} \begin{pmatrix} J_e & 1 & J_i \\ -m & 0 & m \end{pmatrix} R(J_e) \right|^2 . \tag{3}$$

$R(J_e)$ are defined by

$$R(J_e) = \sum_{n_e} \frac{\langle n_f J_f | |r^{(1)}| | n_e J_e \rangle \langle n_e J_e | |r^{(1)}| | n_i J_i \rangle}{E_{n_e} - E_{n_i} - h\nu + i(\Gamma_e/2)},$$

where $\langle n_f J_f | |r^{(1)}| | n_e J_e \rangle$ and $\langle n_e J_e | |r^{(1)}| | n_i J_i \rangle$ are the reduced matrix elements of the transition dipole moment. In Eq. (3), the evaluation of $R(J_e)$ seems necessary. However, Eq. (3) can be transformed into

$$\begin{aligned} P_k = \sum_{RT} \sum_{J_e J_e'} & (-1)^{J_f + J_i} R(J_e) R^*(J_e') (2R+1)(2T+1) \\ & \times \sqrt{2k+1} \begin{Bmatrix} J_i & J_i & k \\ T & R & J_f \end{Bmatrix} \begin{Bmatrix} J_i & J_f & R \\ 1 & 1 & J_e \end{Bmatrix} \\ & \times \begin{Bmatrix} J_i & J_f & T \\ 1 & 1 & J_e' \end{Bmatrix} \begin{pmatrix} 1 & 1 & T \\ 0 & 0 & 0 \end{pmatrix} \begin{pmatrix} 1 & 1 & R \\ 0 & 0 & 0 \end{pmatrix} \\ & \times \begin{pmatrix} T & R & k \\ 0 & 0 & 0 \end{pmatrix}, \end{aligned}$$

where $\{:::\}$ are $6j$ symbols. From this equation it is readily recognized that the ratios $P_0{:}P_2{:}P_4$ are invariant to the relative values of $R(J_e)$ for $J_i \neq J_f$. For the probing scheme we have used, it can be shown that the ratios are $P_0{:}P_2{:}P_4 = 1{:}0.68{:}-0.11$. Therefore, for $J_i \neq J_f$, it is not necessary to evaluate $R(J_e)$. For $J_i = J_f$, the ratios must be calculated numerically.

The $\boldsymbol{v}$-$\boldsymbol{J}$ correlation is naturally expressed in a velocity-fixed (VF) frame where the Z axis is defined along the recoil velocity vector. In this frame, m is defined as so-called helicity (the projection of angular momentum onto the velocity). For simplification of the analysis, we have made two assumptions for angular momentum distribution in the VF frame: (1) the distribution is cylindrically symmetric around the velocity, and (2) the distribution is independent of scattering angle (θ_t, ϕ_t). With these assumptions, the multipole moments in the VF frame are expressed as follows:

$$\rho_0^{(k)}(\mathrm{VF}) = \sum_m (-1)^{J_i - m} \sqrt{2k+1} \begin{pmatrix} J_i & k & J_i \\ -m & 0 & m \end{pmatrix} f_m,$$

where f_m is a fractional population in each m state in the VF frame. The multipole moments in the VF frame can be transformed to those in the PR frame directly, VF $\rightarrow$ PR, or sequentially, VF $\rightarrow$ SF $\rightarrow$ PR. In the latter approach, the multipole moments in the SF frame can be multiplied with a differential cross section [Eq. (1)] for each scattering angle (θ_t, ϕ_t) and then transformed to the PR frame.

The experimental data were analyzed with a forward-convolution method by considering two velocity components with different m distributions. We have assumed that there is no orientation of $\boldsymbol{J}$ in the VF coordinate, so that the angular momentum distribution is characterized by the ratio for $|m| = 0{:}1{:}2$. The calculated images are shown in Figs. 1(a′)–1(d′) and the parameters used are tabulated in Table I.

Although OCS is linear in the ground electronic state, it can be bent in excited states by Renner-Teller interactions. In fact, the major component in the 223 nm photoabsorption of OCS is assigned to the transition to the Renner-Teller A' component of a $^1\Delta$ state [21]. For the lower symmetry of the bent states (C_s point group), symmetry species can be classified as either A' or A'' according to whether it is symmetric or antisymmetric for reflection by the molecular plane. The electronic state of the counterpart fragment CO $X(^1\Sigma^+)$ is classified as A'. Therefore, the overall symmetry of the asymptotic state

TABLE I. Parameters used for the simulation shown in Fig. 1.

					f_m m distribution (VF)[b]		
Dissociation component	Branching ratio	β	E_0[a]	σ[a]	$m = 0$	± 1	± 2
1	1.0	1.8	5.3	4.1	0.60	0.14	0.06
2	3.0	0.7	13.8	5.7	0.48	0.24	0.02

[a]Energy units are in kcal/mol. The translational energy distributions were expressed by Gaussian functions $\sigma^{-1}\sqrt{2/\pi}\,\exp[-2(E - E_0)^2/\sigma^2]$.

[b]The distributions are normalized so that $\sum_{m=-2}^{2} f_m = 1$.

is determined by the symmetry of the S($^1D_2$) atom. To discuss the symmetry of the S atom, another coordinate frame (MS, molecular symmetry) where the Z axis is defined perpendicular to the molecular plane is more useful. In the MS frame, $^1D_2$ states with $m = 0, \pm 2$ belong to A' symmetry, whereas those with $m = \pm 1$ belong to A''. The m distribution in the MS frame, obtained from the distribution in the VF frame, is shown in Table II. The result indicates that 80% of the asymptotic states are in A' symmetry. Although the result suggests different degrees of alignment for the two dissociation components, the present experimental method using two-dimensional imaging and forward-convolution fitting does not allow us to be certain that the difference is significant.

Since the anisotropy parameter is 1.8, the photoabsorption process responsible for the slow component is almost pure $A' \leftarrow A'$. The A'' component manifested by the population in $m = \pm 1$ state in the MS frame may be ascribed to Coriolis coupling in the dissociation process, however, further investigation is necessary. It is pointed out that the total angular momentum in the system is small since the rotational temperature of OCS in a supersonic molecular beam is expected to be very low.

This study has presented experimental and theoretical methods to determine the recoil velocity and alignment of atomic fragments simultaneously. A more rigorous analysis without the simplification we made and also a new experimental approach using 3D imaging [11] are expected to provide a further detailed picture of stereochemical dynamics.

The financial supports by Grant-in-Aid for Scientific Research from the Ministry of Education, Science, Sports and Culture (No. 05237105, No. 07640693, No. 07248231), Morino Foundation, Sumitomo Foundation, and Research Foundation for Opto-Science and Technology are greatly acknowledged.

TABLE II. The m distribution in the MS (molecular symmetry) frame.

	f_m m distribution (MS)[a]		
Dissociation component	$m = 0$	± 1	± 2
1	0.20	0.10	0.30
2	0.14	0.13	0.30

[a]The distributions are normalized so that $\sum_{m=-2}^{2} f_m = 1$.

*Permanent address: Department of Chemistry, Emory University, Atlanta, Georgia 30322.

[1] J. P. Simons, J. Phys. Chem. **91**, 5378 (1987).
[2] P. L. Houston, J. Phys. Chem. **91**, 5388 (1987).
[3] B. J. Van Brunt and R. N. Zare, J. Chem. Phys. **48**, 4304 (1968).
[4] E. W. Rothe, U. Krause, and R. Düren, Chem. Phys. Lett. **72**, 100 (1980).
[5] J. Vigué, J. A. Beswick, and M. Broyer, J. Phys. (Paris) **44**, 1225 (1983).
[6] A. G. Evseev, D. V. Kupriyanov, B. V. Picheyev, B. N. Sevastianov, and O. S. Vasyutinskii, Chem. Phys. **171**, 45 (1993).
[7] B. Ji, P. D. Kleiber, W. C. Stwalley, A. Yiannopoulou, A. M. Lyyra, and P. S. Julienne, J. Chem. Phys. **102**, 2440 (1995).
[8] H. Kato, Faraday Discuss. Chem. Soc. **82**, 1 (1986).
[9] Y. Wang, H.-P. Loock, J. Cao, and C. X. W. Qian, J. Chem. Phys. **102**, 808 (1995).
[10] D. W. Chandler and P. L. Houston, J. Chem. Phys. **87**, 1445 (1987).
[11] K. Tonokura and T. Suzuki, Chem. Phys. Lett. **224**, 1 (1994).
[12] P. L. Houston (private communication); A. G. Suits, R. L. Miller, and P. L. Houston (unpublished).
[13] T. Suzuki, H. Katayanagi, Y. Mo, and K. Tonokura, Chem. Phys. Lett. (to be published).
[14] H. Katayanagi, Y. Mo, and T. Suzuki, Chem. Phys. Lett. **247**, 571 (1995).
[15] A. G. Suits, R. L. Miller, L. S. Bontuyan, and P. L. Houston, J. Chem. Soc. Faraday Trans. **89**, 1443 (1993).
[16] K. Blum, *Density Matrix Theory and Applications* (Plenum, New York, 1981).
[17] R. N. Zare, *Angular Momentum* (Wiley, New York, 1988).
[18] U. Fano and J. H. Macek, Rev. Mod. Phys. **45**, 553 (1973).
[19] D. A. Case, G. M. McClelland, and D. R. Herschbach, Mol. Phys. **35**, 541 (1978).
[20] A. C. Kummel, G. O. Sitz, and R. N. Zare, J. Chem. Phys. **85**, 6874 (1986).
[21] M. Rokutan and S. Iwata (private communication).